2014 IEEE 11th International Conference on Mobile Ad Hoc and Sensor Systems

Multi Channel Performance of Dual Band Low Power Wireless Network

Shengrong Yin, Omprakash Gnawali
Department of Computer Science
University of Houston
{syin, gnawali}@cs.uh.edu

Philipp Sommer, Branislav Kusy
CSIRO Autonomous Systems
Brisbane, QLD, Australia
{philipp.sommer, brano.kusy}@csiro.au

***Abstract*—Wireless sensor network platforms share the wireless communication channels with Wi-Fi and Bluetooth based networks, resulting in heavy use of these bands. As a consequence, platforms in wireless sensor networks need to carefully consider external interference to achieve reliable communication. In this paper, we present an experimental analysis of wireless channels for wireless sensor network operating on dual frequency bands. Specifically, we designed a set of detailed experiments aiming to find out correlation patterns in 900 MHz and 2.4 GHz ISM bands. We conducted our experiments on two testbeds and investigated the band correlation between two distinctive radio transceivers in two different office-space environments. From our data samples, we quantified frequency channel and band correlations in parallel experiments that eliminate artifacts stemming from different external activity on the test site. We found that network formed in 900 MHz band has 15% more connectivity than network formed in 2.4 GHz band, even on radio channels that minimize overlap with Wi-Fi networks.**

***Index Terms*—wireless channel, low power wireless network, dual band, wireless sensor network**

I. Introduction

Low power wireless communication is the basic building block of wireless sensor networks. Applications for wireless sensor networks apply to human daily lives ranging from medical care to smart agriculture and have been developing at a fast pace. The ever more crowded wireless spectrum and the associated communication reliability and robustness problems, however, have started to have an impact on the uptake of wireless sensor network platforms by the industry. We argue that a better understanding of low power wireless, based on detailed physical and link layer measurements, is necessary to improve the network reliability.

Srinivasan et al [1] present that mismatch between abstraction and reality in low power wireless has been a tremendous impediment for protocol designers. One of the main reasons is that link layer performance of radios, conditional to different modulation schemes, transmission powers, and operating frequencies, is rarely understood at a sufficient detail. The network and link layer decisions of when, at what power, and with which neighbor to communicate is a complex decision due to the dynamic and unstable characteristics of the low power wireless links. Nevertheless, network protocols can greatly benefit from utilizing high quality wireless links in terms of energy efficiency of the network as a whole, improved network lifetime, and robustness of the wireless sensor network.

Commoditization of low power wireless technology has led to a decrease in the cost of hardware components. Several platforms and testbeds exist that offer wireless communication at multiple frequency bands. Because multi-radio wireless sensor network platforms are relatively new, the underlying performance of radio communication on different channels and correlation of radio links across multiple bands are not well understood. This measurement study aims to provide network protocol designers and practitioners with detailed performance evaluation of multi-band and multi-channel radio communications. We present evaluation of 900 MHz and 2.4 GHz wireless links operating simultaneously on two different testbeds located in office-like environments.

In addition to studying correlation of two different radio bands, we also study the impact of external interference on low-power wireless links. Our testbeds exhibit different external interference patterns due to their locations in countries (USA and Australia) which may have different patterns of use in the two bands. Some of the major external interference sources in 2.4 GHz band are common around the world, due to the widespread use of technologies in our offices and households, such as Wi-Fi, Bluetooth, and Zigbee. On the other hand, the 900 MHz frequency band is mostly used for proprietary low duty-cycle communications and is not as likely to record significant external interference. Less external interference allows for reliable transmissions with fewer retries, which helps to save battery power.

Increasing popularity of multi-band communication has triggered studies on the benefits of multi-radio technology. Kusy et al. [2] found that network reliability can be significantly improved by using dual radio communication. They compared the performance of dual-band with single-band communication on a 30-node testbed and concluded that dual radio communication can help increase the network throughput without having a significant impact on energy-efficiency. However, this work is based on measurements at the network layer, which differs from our investigations of the link layers. Our study is based on two different dual radio testbeds which helps us eliminate the impact of local climate and external interference environment on the performance of wireless radio links. Our experimental setup allows us to run experiments on multiple channels simultaneously, improving scalability of our experiments.

978-1-4799-6036-1/14 $31.00 © 2014 IEEE
DOI 10.1109/MASS.2014.120

Our main contributions are as follows:

- We present detailed channel measurements on a large scale dual-band testbed.
- We present experimental results showing that 900 MHz band provides more reliable connectivity compared to the 2.4 GHz band, especially on radio channels that experience high levels of 802.11 interference.
- We present a study of the temporal properties of simultaneously operating dual bands.

II. Related Work

Wireless sensor networks are used in various application domains in cyber physical systems. They typically use unlicensed bands of the wireless spectrum. However, the unlicensed spectrum band is shared with other technologies such as Wi-Fi or Bluetooth which can have a severe impact on the performance of wireless links between sensor nodes. Therefore, mitigation of channel interference and coexistence of several technologies in a shared wireless spectrum have been studied intensively in recent years. In the following, we provide an overview of prior research undertaken to improve the understanding of the wireless channels in both the 900 MHz and 2.4 GHz frequency bands.

Wireless Measurements of the 2.4 GHz Band. Lee et al. [3] sampled the chip's RSSI register at 1 kHz using the TI CC2420 transceiver in controlled areas. They found noise patterns with temporal variations and proposed a model to simulate packet delivery based on different noise signatures from empirical measurements.

Rusak and Levis [4] performed experimental study and understand and model the wireless channel. They found that bursts occur at longer time-scales of the wireless measurement either.

Srinivasan et al. [5] studied packet reception in 802.15.4 channels and proposed a quantification metric for the link burstiness (β-factor). More recently, Srinivasan et al. [1] presented a conceptual model of wireless networks and used empirical measurements for TelosB and MicaZ nodes to validate or dispute the claims in the proposed model. They observed 802.11b interference at 45 dB above the noise floor and suggested avoiding channels that coexist with Wi-Fi networks.

Sha et al. [6] performed wireless measurements in the 2.4 GHz band across multiple channels in a wireless sensor network deployed in residential environments. They found significant temporal and spatial variations in quality of channels. They also reported that 2.4 GHz channels exhibit non-periodic noise. Hermans et al. [7] improved packet reception ratios under heavy interference from 45% to 61% by classifying corrupted packets in unique patterns using machine learning. Boano et al. [8] proposed the JamLab testbed to regenerate precise interference patterns using a low-cost infrastructure to evaluate the performance of existing sensor network protocols under interference in the 2.4 GHz band. Noda et al. [9] presented a new channel quality metric to quantify spectrum usage based on the availability of the channel over time.

Wireless Measurements of the 900 MHz Band. Boers et al. [10] exploited the method to classify the interference exist in the wireless channels of the 904 to 928 MHz ISM band, which provided us some insight to investigate the pattern of interference in 900 MHz band, especially in office-like environment. Incel et al. [11] studied how transmission on one channel can cause interference on neighboring channels. They used a platform with a radio transceiver operating in the 868/915 MHz ISM band.

Multi-Band Wireless Measurements. There are a few wireless sensor network testbeds on which we can perform multi-band wireless measurements. Handziski et al. [12] presented TWIST, a scalable and flexible testbed architecture for indoor deployment of wireless sensor networks. They deployed two platforms on TWIST: 102 TmoteSky nodes working on 2.4 GHz band and 102 eyesIFX nodes working in 868 MHz band. Each node uses one transceiver in one band. Using Fleck nodes, a predecessor to the Opal [13] platform using the same radio transceivers, Kusy et al. [2] perform empirical experiments on a testbed of 30 nodes to compare the CTP performance under single and dual radio settings. Opal and Fleck nodes have two transceivers operating in the 900 MHz and 2.4 GHz bands. These prior experiments mainly study the network layer performance. Unlike those studies, our goal is to understand the physical/link layer performance under simultaneous dual radio communication.

Lim et al. [14] developed the Flocklab testbed for distributed, synchronized tracing and profiling of wireless embedded systems. This testbed has four types of nodes: Tmote Sky, IRIS, Opal and Tinynode. Thus one could perform multi-band measurements on this testbed. In our study, we use Twonet testbed [15] and a 17-node testbed of Opal nodes at CSIRO.

III. Experimental Setting

We describe the experimental setup used for this dual-band wireless channel measurement study.

A. Platform

Opal: The Opal platform [13] was developed by CSIRO to provide wireless channel diversity by using two radio transceivers operating in different bands. It embeds an Atmel ARM Cortex-M3 low-power MCU and two radios: the Atmel AT86RF212 transceiver (900 MHz) and the AT86RF231 (2.4 GHz) transceiver. Each radio uses a separate antenna matched to the RF frequency.

AT86RF231: The Atmel AT86RF231 [16] is a low-power 2.4 GHz radio transceiver designed for IEEE 802.15.4 applications. The AT86RF231 is suitable for applications in wireless sensor networks that operate in the 2.4 GHz band. Like the popular TI CC2420 radio, Atmel's RF231 also supports 16 channels in the 2.4 GHz band with a channel spacing of 5 MHz. The center frequency F_c of these channels is defined as follows:

$$F_c = 2405 + 5 * (k - 11)[MHz], k = 11, ..., 26 \quad (1)$$

TABLE I
COMPARISON OF TRANSCEIVER CONFIGURATIONS

Transceiver	Range	Resolution	Sensitivity	TX Power	Modulation	Trans. Rate	Channels	Frequency
RF231	81 dBm	3 dBm	-91 dBm	3 dBm	OQPSK	250kbps	11-26	2.4-2.485 GHz
RF212	87 dBm	3 dBm	-98 dBm	3 dBm	OQPSK	250kbps	1-10	906-924 MHz

where k is the channel number from 11 to 26.

The AT86RF231 can update the RSSI register every 2 μs and the readings are in the range between 0 and 28. A register value of 0 indicates a RF input power of less than -91 dBm [16]. For a register value ranging from 1 to 28, we can compute the corresponding RF power as follows:

$$RSSI(dBm) = -91 + 3 * (R - 1) \quad (2)$$

Here R indicates the raw register value. The RF231 transceiver has a minimum RF sensitivity of -91 dBm.

AT86RF212: The Atmel AT86RF212 [17] is a low-power, low-voltage 700/800/900 MHz transceiver designed for the IEEE 802.15.4 standard and high data rate ISM applications. For the sub-1 GHz bands, it supports multiple data rates (20, 40, 100, 200, 250, 500, and 1000 kbps). In our experiments, we configured both the radios to use OQPSK modulation and 250kbps data rate. There are 10 channels in the North American ISM band from 902 to 928 MHz with a channel spacing of 2 MHz according to IEEE 802.15.4-2003/2006. The center frequency of these channels is defined as:

$$F_c = 906 + 2 * (k - 1)[MHz], k = 1, 2, ..., 10 \quad (3)$$

where k is the channel number from 1 to 10.

Under the OQPSK modulation, the RF212 transceiver can update the RSSI value every 8 μs. Similar to the RF231 radio, RSSI readings have a resolution of 3 dBm and the register value ranges from 0 to 28. An RSSI value of 0 indicates an RF input power is equal or less than the minimum RF sensitivity, which is -98 dBm for OQPSK [17]. For a RSSI value ranging from 1 to 28, we can use the following formula to calculate the RF power:

$$RSSI(dBm) = -98 + 3.1 * (R) \quad (4)$$

Table I summarizes the transceiver settings used during the experiments.

B. Testbeds

We conducted our experiments on two testbeds.

Twonet: Twonet is a large-scale wireless sensor network testbed deployed at the Phillip G. Hoffman Hall at the University of Houston. The testbed consists of 100 Opal nodes which are connected to a network of 20 Raspberry Pi nodes, which are connected to a server [15]. The Opal nodes are deployed across four floors of the building.

CSIRO testbed: The indoor testbed deployed at CSIRO consists of 17 Opal nodes distributed over two adjacent wings of a large building, which includes offices, storage areas and laboratories. Each Opal node is attached to a PandaBoard embedded Linux PC, which provides an Ethernet-based backchannel to a central server for logging serial output.

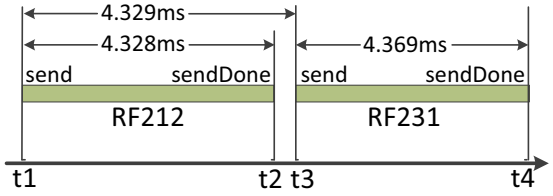

Fig. 1. Packet transmission timing in the two bands during our experiments.

C. Metrics

In our experiments, we perform channel measurements by letting each node on the testbed transmit radio packets every 10 seconds and receive all the packets transmitted by other nodes. There is a low probability that two nodes transmit at the same time due to randomization and jitter in the transmit logic. We read RSSI for each received packet and use the sequence numbers embedded in the packet to calculate the packet reception ratio on a specific link. We pick the following two metrics to evaluate the experimental data gathered on the two testbeds.

Received Signal Strength Indicator (RSSI). We can read RSSI values directly from the radio transceivers. The RSSI is a combination of the received radio signal and the noise floor/interference at the receiver. Even if there is no packet currently being received by the receiver, we can still capture RSSI readings to sample the background noise of the environment.

Packet Reception Ratio (PRR). The Packet Reception Ratio (PRR) represents the success rate for link-layer packet transmissions between a sender-receiver pair. This metric is frequently used to assess the quality of links and to predict the performance of higher layer protocols.

D. Concurrent Transmissions in Two Bands

Although we use the phrase *concurrent transmission in two bands* in this study, the packets are not transmitted concurrently in the two bands. In our experiments, the mote transmits a packet using one radio. Immediately after the completion of this transmission, the node transmits a packet using the second radio. Figure 1 shows the average packet

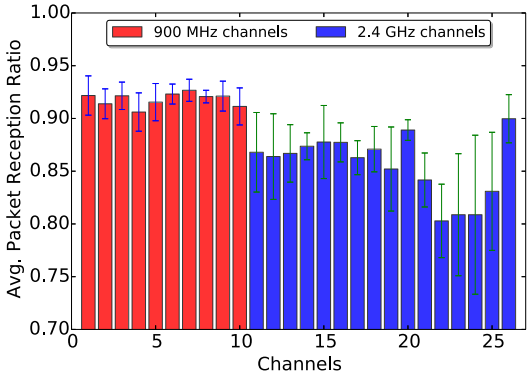

Fig. 2. Average PRR over three repeated experiments across all 100 nodes scanning all channels on Twonet).

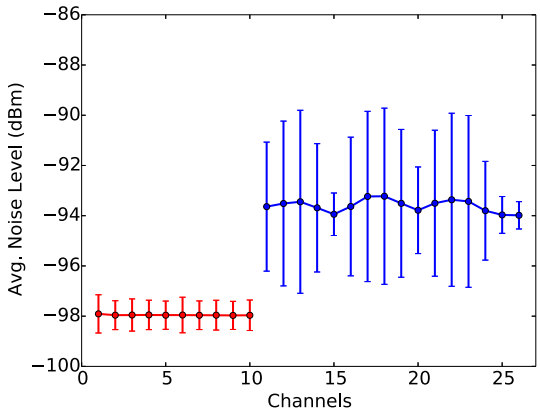

Fig. 3. Average sampled signal strength over two experiments across 16 nodes on Twonet.

TABLE II
NODE-CHANNEL ASSIGNMENT PATTERN USED FOR CONCURRENT MEASUREMENTS ON 4 CHANNELS

Node ID	1	2	3	4	...
Channels	(6,16)	(10,26)	(6,16)	(10,26)	...

transmission timing on the two radios and the time between the two transmissions. RF212 takes an average of 4.328ms to send a packet. RF231 takes an average of 4.369ms to send a packet. There is approximately 1 μs time interval between the sendDone event from RF212 and the send call to RF231. Thus, the motes transmit the packets nearly concurrently in the two bands.

E. Measurement Campaigns

We wrote a TinyOS application that transmits a packet every 10 seconds with both the transceivers at the same time. The application logs all the packets received. The motes also record receive and transmit timestamps and RSSI readings. The motes send all the captured data to the server which manages and configures the status of the testbed.

To measure PRR across all the channels on the testbed, we do the following experiment. The motes transmit/receive packets and sample noise in the two bands simultaneously, using one channel from the 2.4 GHz band (RF231) and one channel from the 900 MHz band (RF212). The motes with even node id sample two channels and the motes with odd node id sample different two channels using the pattern shown in Table II. Thus, we perform packet and channel measurement on four channels concurrently. This methodology provides channel diversity without losing the experiment scalability. We configure the radios to use the settings in Table I. Each measurement campaign lasts 60 mins, during which each mote transmits 720 packets (360 on each channel). We repeat each experiment three times. We performed these measurements at night when the spectrum is quiet without human activity.

IV. MEASUREMENT RESULTS

In this section, we present the results from our detailed measurements of multiple channels on multiple testbeds. Overall, we find that 900 MHz band can provide 15% more connectivity compared to the 2.4 GHz band on our testbeds.

A. Performance Across 900 MHz and 2.4 GHz Bands

Fig. 2 shows the average PRR across all channels in the two bands on Twonet. We can see 900 MHz channels provides better PRRs compared with 2.4 GHz channels. 2.4 GHz channels are quite busy on our testbed. This is a somewhat expected result and also reported in previous work. The main difference is our observations are from concurrent channel sampling. Overall, the links on 900 MHz channels have average PRR of 91.82% (max was 92.67% and min was 90.61%) and the links on 2.4 GHz have average PRR of 85.59% (max was 89.97% and min was 80.29%) during our measurement campaigns.

Each testbed environment may be different and hence the level of noise, which could be one explanation for the difference in PRRs across the testbed. To sample noise across all the channels and locations on the testbed, we run an experiment cycling through all 900 MHz and 2.4 GHz channels using a technique called channel scanning [18]. Fig. 3 shows the data from the measurement. We find that 900 MHz channels are quieter than the 2.4 GHz channels. Particularly, in the 2.4 GHz band, channels 15, 20, 25, 26 are Wi-Fi free channels. Thus, these channels have less variable noise than other channels. We observe lower noise and variation on the 900 MHz channels. This is despite their overlap with GSM signals [2]. Our guess is these signals or devices that use 900 MHz are not a big factor in the building where Twonet is deployed.

B. Distribution of Packet Reception Ratio

Figure 4 shows how PRR is distributed across the Twonet testbed and the CSIRO testbed. The color of each (x,y) cell indicates the PRR for the corresponding node-pair x and y. The first observation is there are more colored cells and darker

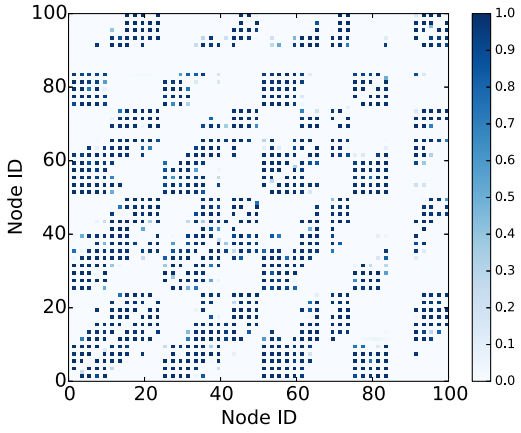

(a) Twonet testbed: PRR on channel 10

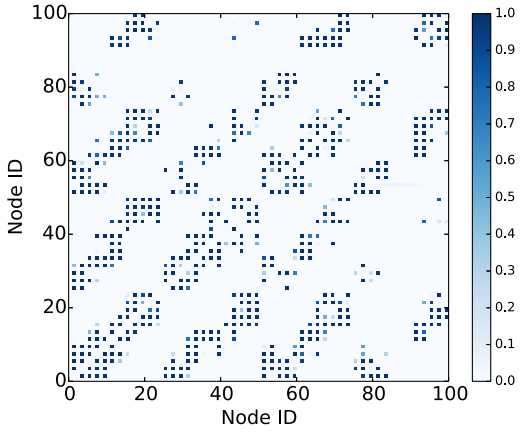

(b) Twonet testbed: PRR on channel 26

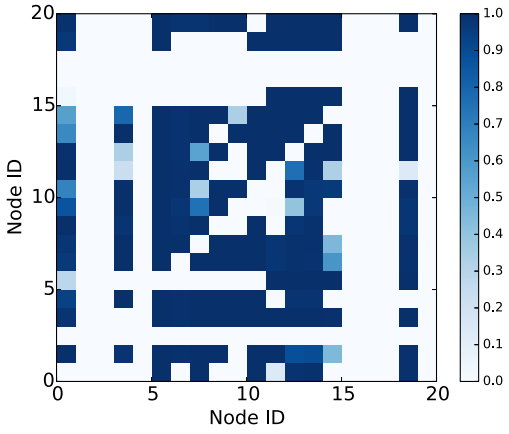

(c) CSIRO Testbed: PRR on channel 10

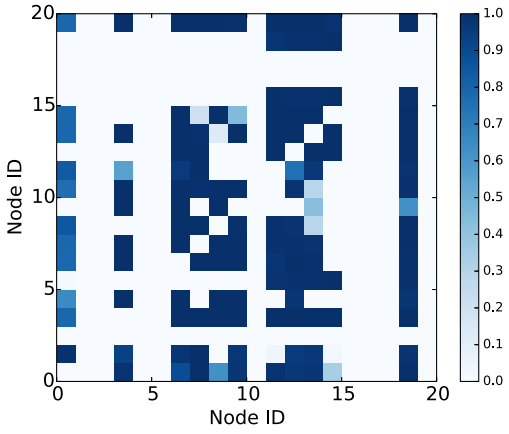

(d) CSIRO Testbed: PRR on Channel 26

Fig. 4. The 900 MHz band provides more connectivity compared with the 2.4 GHz band both on Twonet and CSIRO testbed. The color displayed on each small square box represents the PRR for the corresponding node pair. Darker color implies higher PRR.

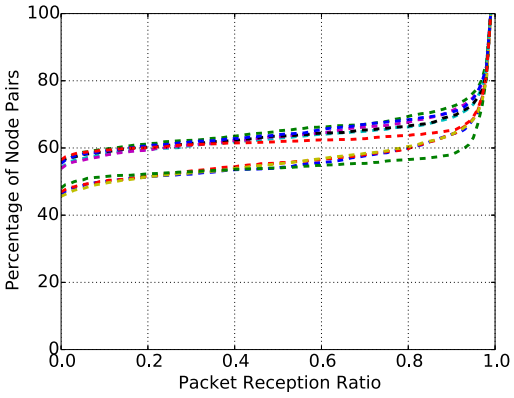

(a) CDFs of PRR for each channel (1 to 10) in 900 MHz band

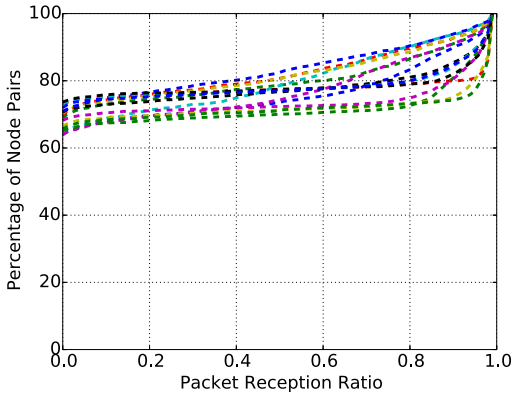

(b) CDFs of PRR for each channel (11 to 26) in 2.4 GHz band

Fig. 5. Comparison of connectivity with 900 MHz and 2.4 GHz channels on Twonet testbed.

colors on PRR heatmap for channel 10 compared to the PRR heatmaps for channel 26. This suggests that there is better connectivity on channel 10 than with channel 26. Traditionally in sensor network literature, channel 26 is reported as the best channel for network formation. Our data shows that channel 10 is even better.

The second observation is the diagonal pattern of the colored cells in Figure 4, especially on the heatmaps for Twonet. The pattern is the result of the deployment topology of the motes on the testbed which results in a specific connectivity pattern. On Twonet, 100 Opal nodes are deployed across four floors of an academic building, with 25 nodes deployed in the ceiling of each floor. Nodes 1-25 are on the third floor. Nodes 26-50 are on the second floor. Nodes 51-75 are on fourth floor. Nodes 76-100 are on fifth floor. On each floor, five Opal nodes, with consecutive node ids, are connected via cables to the same USB hub. Although cables of different lengths are used to separate them as far apart as possible, the motes naturally form spatial clusters around the USB hub. Hence, nodes closer in node ids are likely to be able to communicate with each other resulting in a large number of colored cells along the diagonal. The figure also has second and third diagonals, each separated by about 25 units to the left and right of the main diagonal connecting the bottom-left to top-right corners. These additional diagonals are due to inter-floor connectivity and the pattern of deployment: the mote ids are sequential on each floor. Thus, nodes 1-5, which are near one corner of the third floor, are likely to be able to communicate directly with nodes 26-30, which are deployed in the same corner but on the second floor. Similarly, nodes 6-10 are likely to have good connectivity to not only the nodes adjacent to it on the same floor but also nodes 31-35 which are on the adjacent floor direct below it. Thus, we get a second diagonal from (0,25) to (75,100). Other diagonals also capture similar geometric information about the deployment within a floor and across the floors. The PRR heatmap for CSIRO testbed does not show similar geometric pattern because the nodes are deployed over a large area within the same floor.

Figure 5 shows the distribution of link PRR across node-pairs for the channels in 900 MHz and 2.4 GHz bands. We find that a large number of node-pairs do not have viable links. With 900 MHz channels, approximately 45-60% of node-pairs are not connected with links. On 2.4 GHz channels, 65-75% of node-pairs are not connected with links. Thus, 900 MHz band provides more connectivity than 2.4 GHz band. We also find that almost 20% of the links are close to 100% PRR in the 900 MHz band. Regardless of the channel, much smaller fraction of nodes have links with close to 100% PRR in the 2.4 GHz band. Another observation is the clustering of PRR distribution for 900 MHz into two distinct bands. We do not understand the reason for this clustering given 900 MHz channels are fairly similar to each other in terms of their PRRs as shown in Figure 2.

Next, we examine the variation in the channel PRRs in the two bands. We sample PRR of channel 10 and channel 21 concurrently for 60 hours on Twonet using the technique

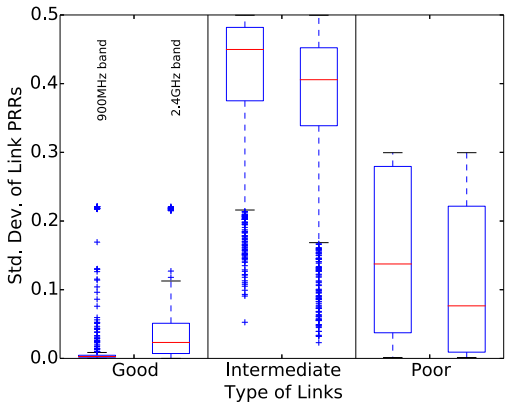

Fig. 6. Boxplot of standard deviation of link PRRs across all the links in 900 MHz band and 2.4 GHz band.

described in Section III. We calculate the PRR for each link over each one-hour interval, sliding the window by 1-hour. Thus, we have 60 PRR values for each link covering 60 hours. Then, we compute the standard deviation of these 60 PRR values as a measure of temporal variation of link PRR. We aggregate the standard deviation of PRR from all the links and divide the dataset into three segments by the average PRR: links with less than 10% PRR (as poor links), links with 10-90% PRR (as intermediate links), and links with greater than 90% PRR (as good links). We plot these standard deviations for the two channels in Figure 6 to study how dynamic the channels in the two bands are. We observe that intermediate quality links are most dynamic, uncorrelated with distance and quite unstable both in 2.4 GHz band and 900 MHz band. Poor quality links show small dynamics than the intermediate links. The good links are the most stable. Our observation regarding the relative stability of good links compared to intermediate links confirms previously reported results [19]. Finally, we also observe that good links in 900 MHz channels are more stable than the good links in 2.4 GHz channels. Overall, we find that 900 MHz channels provide more connectivity that is more stable over time compared to the channels in 2.4 GHz band.

Different testbeds have different PRR distribution due to their deployment topology and physical environment. Figure 7 shows the PRR across two bands across two testbeds. We collect link PRR on Twonet and CSIRO testbeds for 24 hours. We show the PRR for all node pairs sorted by the PRR on channel 26 in Figure 7(a) and 7(b). This figure allows us to compare the PRR on channel 10 and channel 26 for a given node pair. On Twonet, the blue dots (PRR on channel 26) is mostly on the bottom-left side of the red dots (PRR on channel 10) suggesting links formed between a given node-pair on channel 10 is better than the link on channel 26 between the same node-pair. On CSIRO, the PRR on channel 10 is still better than the PRR on channel 26 but the difference is not as large as it is on Twonet. We summarize this dataset using CDF on Figure 7(c) and 7(d). Channel 10 in the 900 MHz band

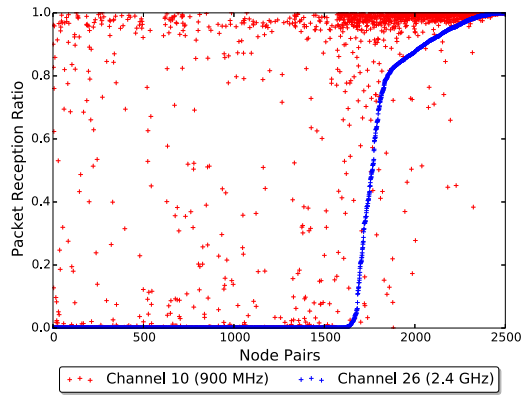

(a) PRR in two bands sorted by PRR on channel 26 on Twonet testbed.

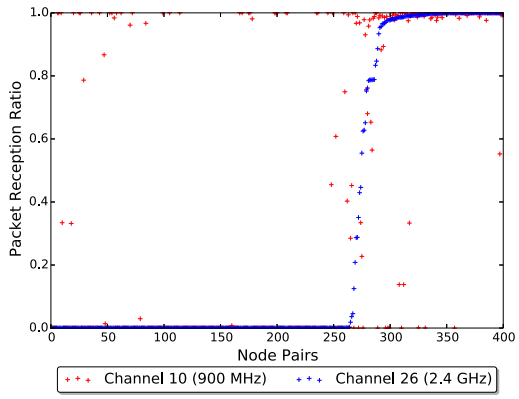

(b) PRR in two bands sorted by PRR on channel 26 on CSIRO testbed.

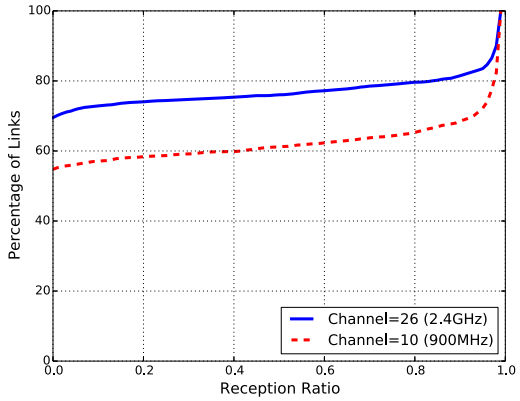

(c) CDFs of PRR for Twonet testbed.

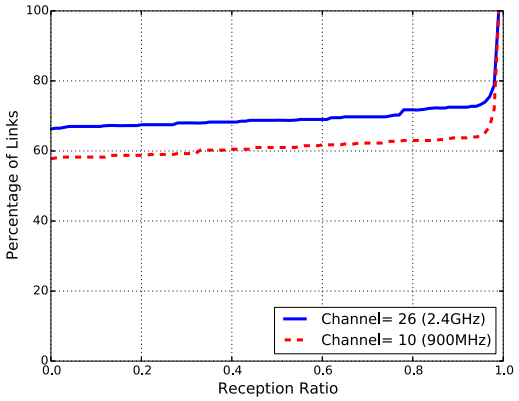

(d) CDFs of PRR for CSIRO testbed.

Fig. 7. Comparison of PRR across the two testbeds in two bands. Higher PRR of 900 MHz channels on both the testbeds.

has 15% more links than Channel 26 on Twonet and around 10% more links on CSIRO Testbeds. Both channels have less than 20% intermediate links on both the testbeds. There are fewer good links (as a fraction of all the links) on Twonet compared to CSIRO in both the bands.

C. Channel Noise and Burstiness

In earlier sections, we studied the long term properties of the channel using measurement probes sent at several second intervals. Now we study the short term properties of the wireless link. The burstiness of the wireless channel in the 2.4 GHz band is dominant especially in the channels that overlap with the Wi-Fi channels, such as channel 16. We extend our observation to not only the burstiness of 2.4 GHz but also the burstiness of 900 MHz at the same time.

To sample noise on the channel, we programmed the nodes to sample the RSSI continuously at 100 Hz. We configured both the radios to run with OQPSK modulation scheme and 250kbps data rate. We sample RSSI on channels 6, 10, 16, and 26 on Twonet testbed for 24 hours collecting almost 2.5 million samples. The channel assignment for the measurement follows the pattern described in Table II. Figure 8 shows the RSSI on the four channels over 24 hours. We observe that channel 6 and 10 have less ambient noise than channels 16 and 26 and confirms the short term observations shown in Figure 3. The noise patterns are largely consistent over the long term. Figure 8(b) shows 1000 noise samples on the four channels. We find that channel 16 is bursty as expected. Rest of the channels are less bursty.

Figure 9 presents the CDFs of RSSI sample values in the four channels sampled concurrently. We find that a large fraction of RSSI samples on channel 16 range from -91dBm to -70dBm, which is 25% of the full dynamic range supported by the RF231 radio. Most RSSI samples on channel 6 fall on a narrower range of -98dBm to -95dBm, which is 3% of the full dynamic range supported by the RF212 radio. For channel 26, the RSSI range is -91dBm to -79dBm, which is 15% of the full dynamic range of the radio. For channel 10, the RSSI range is -98 dBm to -92 dBm, which is about 7% of the full dynamic range of the radio. We summarize these results in Table III.

Next we study how often these bursts occur in the channels.

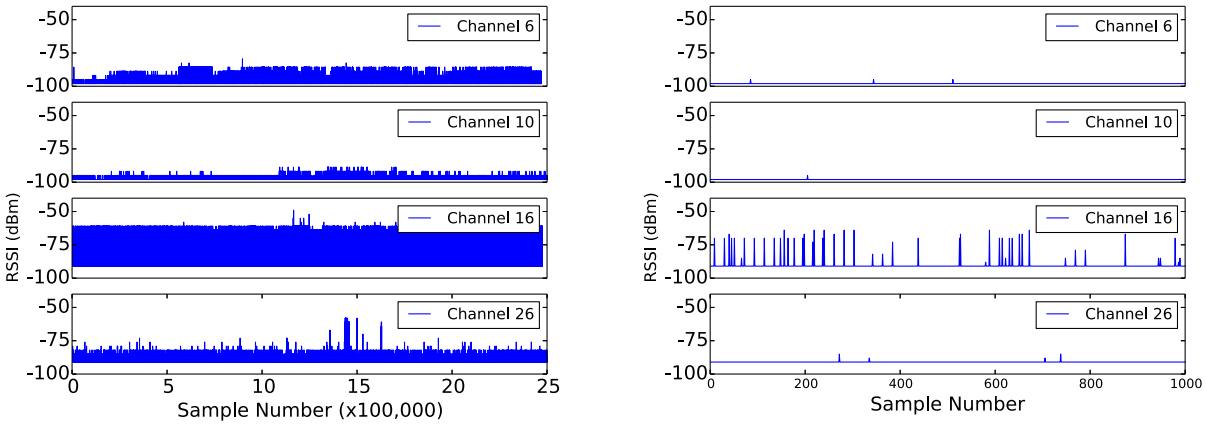

(a) RSSI traces over 24 hours

(b) RSSI traces over 10 seconds

Fig. 8. RSSI samples on four channels

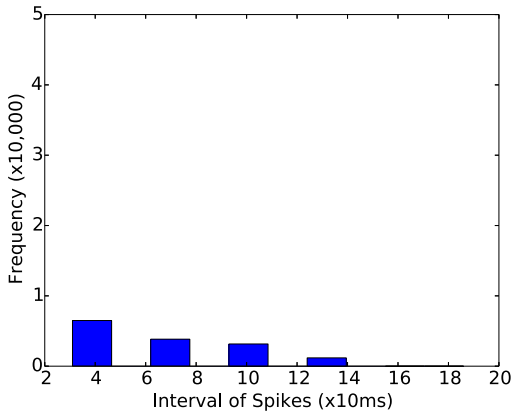

Fig. 10. Spike interval distribution on channel 6 on Twonet testbed.

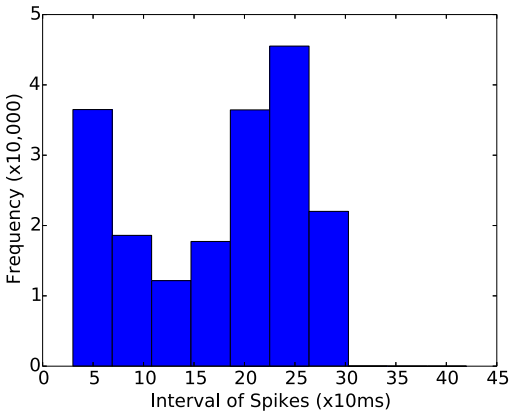

Fig. 11. Spike interval distribution on channel 16 on Twonet testbed.

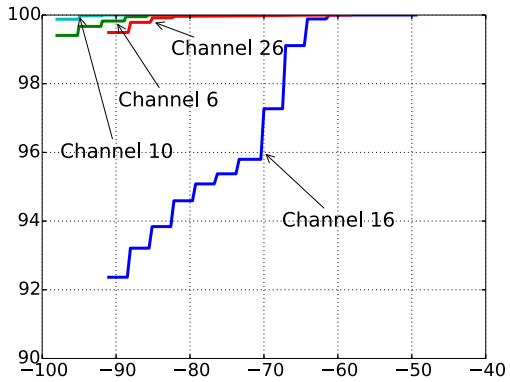

Fig. 9. CDFs of noise level for four channels in two bands.

TABLE III
SUMMARY OF RSSI DISTRIBUTIONS IN TWO BANDS

Channel	6	10	16	26
Band	900 MHz	900 MHz	2.4 GHz	2.4 GHz
Avg. of RSSI (dBm)	-97.997	-97.994	-90.604	-90.984
Std. of RSSI (dBm)	0.0997	0.142	2.237	0.260

We define a spike as a sample which is larger than the minimum sensitivity of the transceivers: -91dBm for RF231 and -98 dBm for RF212. We then compute the interval between the spikes and plot the histogram in Figure 10 and Figure 11 after filtering the intervals larger than 450 ms. The figure shows that the spikes on channel 6 (avg. 60 ms) occur more frequently than in channel 16 (avg. 170 ms) when observed through our 100 Hz probes.

V. Conclusions

In this paper, we presented results from our study of the 900 MHz and 2.4 GHz bands typically used in low power wireless networks. We found that the 900 MHz band provides 15% more connectivity compared with the 2.4 GHz band. Compared to prior work that has also done some studies of these two bands, we made concurrent measurements on multiple channels. Based on the insights from our work, one could design protocols to increase network reliability by taking advantage of the two bands. We performed our measurements on two different testbeds, which gives us confidence about the validity of the results.

Acknowledgment

We thank Qiang Li for his initial deployment of Twonet and inspiring discussions about the testbed debug issues. This work was partially supported by the National Science Foundation under grant no. IIS-1111507.

References

[1] K. Srinivasan, P. Dutta, A. Tavakoli, and P. Levis, "An empirical study of low-power wireless," *ACM Transactions on Sensor Networks (TOSN)*, vol. 6, no. 2, p. 16, 2010.

[2] B. Kusy, C. Richter, W. Hu, M. Afanasyev, R. Jurdak, M. Brunig, D. Abbott, C. Huynh, and D. Ostry, "Radio diversity for reliable communication in wsns," in *Proceedings of the 10th International Conference on Information Processing in Sensor Networks (IPSN)*, April 2011, pp. 270–281.

[3] H. Lee, A. Cerpa, and P. Levis, "Improving wireless simulation through noise modeling," in *Proceedings of the 6th International Symposium on Information Processing in Sensor Networks (IPSN)*, 2007, pp. 21–30.

[4] T. Rusak and P. Levis, "Burstiness and scaling in the structure of low-power wireless links," *Mobile Computing and Communications Review*, vol. 13, no. 1, pp. 60–64, 2009.

[5] K. Srinivasan, M. A. Kazandjieva, S. Agarwal, and P. Levis, "The β-factor: measuring wireless link burstiness," in *Proceedings of the 6th ACM conference on Embedded network sensor systems (SenSys)*, 2008, pp. 29–42.

[6] M. Sha, G. Hackmann, and C. Lu, "Multi-channel reliability and spectrum usage in real homes: empirical studies for home-area sensor networks," in *Proceedings of the Nineteenth International Workshop on Quality of Service (IWQoS)*, 2011, pp. 39:1–39:9.

[7] F. Hermans, O. Rensfelt, T. Voigt, E. Ngai, L.-A. Norden, and P. Gunningberg, "Sonic: classifying interference in 802.15.4 sensor networks," in *Proceedings of the 12th international conference on Information processing in sensor networks (IPSN)*, 2013, pp. 55–66.

[8] C. Boano, T. Voigt, C. Noda, K. Romer, and M. Zuniga, "Jamlab: Augmenting sensornet testbeds with realistic and controlled interference generation," in *10th International Conference on Information Processing in Sensor Networks (IPSN)*, 2011, pp. 175–186.

[9] C. Noda, S. Prabh, M. Alves, C. A. Boano, and T. Voigt, "Quantifying the channel quality for interference-aware wireless sensor networks," *SIGBED Rev.*, vol. 8, no. 4, pp. 43–48, Dec. 2011.

[10] N. M. Boers, I. Nikolaidis, and P. Gburzynski, "Sampling and classifying interference patterns in a wireless sensor network," *ACM Transactions on Sensor Networks (TOSN)*, vol. 9, no. 1, p. 2, 2012.

[11] O. D. Incel, S. Dulman, P. Jansen, and S. Mullender, "Multi-channel interference measurements for wireless sensor networks," in *Proceedings of the 31st IEEE Conference on Local Computer Networks (LCN)*, 2006, pp. 694–701.

[12] V. Handziski, A. Köpke, A. Willig, and A. Wolisz, "Twist: a scalable and reconfigurable testbed for wireless indoor experiments with sensor networks," in *Proceedings of the 2nd international workshop on Multi-hop ad hoc networks: from theory to reality*. ACM, 2006, pp. 63–70.

[13] R. Jurdak, K. Klues, B. Kusy, C. Richter, K. Langendoen, and M. Brunig, "Opal: a multiradio platform for high throughput wireless sensor networks," *IEEE Embedded Systems Letters*, vol. 3, no. 4, pp. 121–124, 2011.

[14] R. Lim, F. Ferrari, M. Zimmerling, C. Walser, P. Sommer, and J. Beutel, "Flocklab: A testbed for distributed, synchronized tracing and profiling of wireless embedded systems," in *Proceedings of the 12th international conference on Information processing in sensor networks*. ACM, 2013, pp. 153–166.

[15] Q. Li, D. Han, O. Gnawali, P. Sommer, and B. Kusy, " Demo Abstract: Twonet - Large-Scale Wireless Sensor Network Testbed with Dual-Radio Nodes ," in *Proceedings of the 11th ACM Conference of Embedded Networked Sensor Systems (Sensys)*, Nov 2013.

[16] "Atmel AT86RF231 Datasheet," http://www.atmel.com/images/doc8111.pdf.

[17] "Atmel AT86RF212 Datasheet," http://www.atmel.com/images/doc8168.pdf.

[18] S. Yin, O. Gnawali, P. Sommer, and B. Kusy, "Concurrent wireless channel survey on dual band sensor network testbed," in *Mobile Adhoc and Sensor Systems (MASS), 2014 IEEE 11th International Conference on*, Oct 2014.

[19] N. Baccour, A. Koubaa, L. Mottola, M. A. Zuniga, H. Youssef, C. A. Boano, and M. Alves, "Radio link quality estimation in wireless sensor networks: a survey," *ACM Transactions on Sensor Networks (TOSN)*, vol. 8, no. 4, p. 34, 2012.